Experimental study of Taylor's hypothesis in a turbulent soap film

Andrew Belmonte,[a] Brian Martin, and Walter I. Goldburg
Department of Physics and Astronomy, University of Pittsburgh, Pittsburgh, Pennsylvania 15260

(Received 29 July 1998; accepted 19 November 1999)

An experimental study of Taylor's hypothesis in a quasi-two-dimensional turbulent soap film is presented. A two-probe laser Doppler velocimeter enables a nonintrusive simultaneous measurement of the velocity at spatially separated points. Using the cross correlation between a pair of points displaced in both space and time, the velocity coherence is measured to be better than 90% for scales less than the integral scale. Taylor's hypothesis is confirmed insofar as the lower moments of the longitudinal velocity difference are equal whether measured with or without invoking the hypothesis. A quantitative study of the decorrelation beyond the integral scale is also presented. © *2000 American Institute of Physics.* [S1070-6631(00)02103-6]

I. INTRODUCTION

In a 1938 paper on the statistics of turbulence, Taylor presented an assumption from which he could infer the spatial structure of a turbulent velocity field from a single point measurement of its temporal fluctuation.[1] This assumption, known as Taylor's hypothesis or the frozen turbulence assumption, relies on the existence of a large mean flow which translates fluctuations past a stationary probe in a time short compared to the turbulent dynamics. The experimental measurements treated by Taylor were made on the turbulence generated behind a stationary grid in a wind tunnel, and his hypothesis has become a standard technique employed in similar experiments which inform our current views on turbulence (see, for example, Refs. 2, 3, and 4). The importance of this hypothesis stems from the fact that most turbulence theories are framed in terms of the spatial structure of the velocity field[2,5].

In practical terms, the limits of Taylor's hypothesis are determined by how large the mean velocity must be relative to the fluctuations. Recently Yakhot[6] has pointed out that the corrections to Taylor's hypothesis could well be of the same order as corrections to the standard model of turbulence, Kolmogorov's 1941 theory.[7,8] However, there is at present no firm theoretical derivation of the hypothesis, and thus no fashion to analyze its reliability, calculate higher order corrections, or predict in what way it will break down. A few theoretical discussions do exist,[9–11] the treatment by Lumley in particular offering corrections to measured spatial gradients due to non-negligible velocity fluctuations.[10] An interesting direction has recently been taken by Hayot and Jayaprakash for the Burgers equation.[12] Still a general theoretical framework is lacking.

There have been many experimental studies of Taylor's hypothesis, all in three-dimensional (3-D) turbulence; a brief overview is given in Sec. II. Here we present experiments performed on the quasi-two-dimensional flow of a soap film. Two-dimensional (2-D) fluid flows occur in many physical situations, mostly due to the effects of rotation or stratification in the atmosphere and ocean.[13] Turbulence in two dimensions (2D) is different from 3D in several ways, largely due to the absence of vortex stretching in 2D.[14] Although Taylor's hypothesis is also important for the study of 2D turbulence, to our knowledge it has never been tested.

It may be helpful at this point to discuss the current view of 2D and 3D turbulence. Unlike three dimensions, the vorticity vector $\vec{\omega}$ in 2D must be perpendicular to the x,y plane of the flow.[5,14] From the 2D Navier–Stokes equation it follows that vorticity cannot be amplified by a velocity gradient, and can only be attenuated by viscous damping. In the inviscid limit, the enstrophy $\Omega = \frac{1}{2}\langle \omega^2 \rangle$ becomes a constant of the motion, in addition to the kinetic energy $K = \frac{1}{2}\langle v^2 \rangle$ as in 3D (the angular brackets designate an appropriate average). Thus in 2-D turbulence two cascades are expected: a *direct* cascade of enstrophy to smaller scales, and an *inverse* cascade of energy to larger scales;[15,17] for decaying 2-D turbulence the inverse cascade is absent.[14,16] In 3-D turbulence there is only an energy cascade from large to small scales, which is related to vorticity amplification via vortex stretching, and which depends on the rate ϵ at which kinetic energy is injected at large scales. In 2D, the energy injected at a scale r_{inj} will be transferred to larger scales and dissipated at the boundaries of the system.[14] For scales $r < r_{\mathrm{inj}}$ down to the dissipative scales, the small-scale velocity fluctuations $\langle |\delta v(r)| \rangle$, which carry little of the energy, are expected to depend on the enstrophy injection rate $\beta \equiv \partial\Omega/\partial t$.[14] This process is nonlocal in k-space.[17]

It seems reasonable to expect the absence of vortex stretching in 2D to increase the likelihood of a fluctuation being transported intact to a downstream point. It also seems that lateral mixing effects, which would introduce or remove other fluctuations into the flow path somewhere along the distance $\Delta x = U_0 \Delta t$, would be a less likely occurrence in 2D than in 3D. In both instances one would expect Taylor's hypothesis $\delta v(\Delta x) = \delta v(U_0 \Delta t)$ to do relatively better in 2D than in 3D. However, it is difficult to estimate the role of spectral nonlocality of the cascades in 2D as compared to

[a]Present address: Department of Mathematics, Pennsylvania State University, University Park, Pennsylvania 16802.

3D, and thus no clear conclusion can be made.

Our experiment uses a laser Doppler velocimeter (LDV) with two probes to nonintrusively examine Taylor's hypothesis in a turbulent soap film. Along with the standard statistical use of this hypothesis, we will consider the coherence of the velocity field as it is advected downstream,[18–23] i.e., that $v(x,t)$ is nearly identical to $v(x+\Delta x, t+(\Delta x/U_0))$, where U_0 is the mean velocity and Δx the distance between the points.[1] For a clear illustration of this, glance ahead to Fig. 3. We will refer to this second equivalence between spatial differences and temporal differences as the *coherence hypothesis*.

This coherence hypothesis is unquestionably an approximation and must fail as Δx becomes large; here we quantify this failure, and relate it to the predictability problem for turbulent flows. We measure the breakdown of the coherence hypothesis via the correlation between two points in the flow, displaced in both position and time. We find nevertheless that the expectation value of the lowest six moments of the longitudinal velocity difference is unaffected by this loss of coherence.

II. PREVIOUS STUDIES OF TAYLOR'S HYPOTHESIS

Taylor's hypothesis has been exposed to many experimental tests in three-dimensional turbulence, and we do not intend to give an exhaustive survey here. These experimental studies can be divided into two broad categories, concerned with either correlations over finite distances[18–23] or local spatial derivatives used in turbulent dissipation estimates.[24–27] It has long been appreciated that the validity of Taylor's frozen turbulence assumption requires the smallness of the turbulent intensity I_t, defined as the ratio of rms velocity fluctuations to the mean flow speed U_0. Additionally, the mean shear rate and the viscous damping must be small in the range of spatial scales Δx being probed. In this section we give a sampling of the sort of work which has been done in 3D; a more detailed discussion of studies with which we directly compare our results is given in Sec. V. The reader is referred to introductory reviews in two recent articles,[26,27] which are somewhat complementary to what is given here.

To test Taylor's hypothesis for velocity correlations over finite distances, one approach is to compare measurements made at a single observation point with measurements made at points displaced downstream. The first such tests were made in a wind tunnel by Favre, Gaviglio, and Dumas.[18,19] The measurements were performed within the turbulent boundary layer of a plate at various I_t up to 15%. They found that Taylor's hypothesis is valid for measurements of the velocity correlation function $R(\Delta x,\tau)=\langle v_1(x_1,t)v_2(x_1+\Delta x, t-\tau)\rangle$ made not too close to the plate. Fisher and Davies[20] made careful measurements of the velocity correlation function $R(\Delta x,\tau)$ in a jet. They found that the relation $\tau=\Delta x/U_0$ was not well satisfied in the mixing region, where I_t is typically $\sim$ 20%. These authors observed, as have many others, that the functional form of R changes with increasing Δx, and that this function is not very sharply peaked, as it would be if the coherence hypothesis were satisfied. Comte-Bellot and Corrsin[22] measured $R(\Delta x,\tau)$ for grid-generated turbulence in a wind tunnel, where both I_t and the mean shear rates are rather small. Though downstream decay causes the maximum value of R vs τ to decrease with increasing Δx, the correlation functions could still be collapsed onto the same functional form.

One of the fundamental effects of turbulence is its enhancement of dissipation, the measurement of which requires knowledge of spatial derivatives. Using Taylor's hypothesis allows the time derivative of a single point measurement to be related to spatial derivatives, the simplest relation being $\partial\phi/\partial t = U_0(\partial\phi/\partial x)$, where ϕ could be a passive scalar concentration, temperature, a velocity component, or a product of velocity components. Kailasneth, Sreenivasan, and Saylor[25] studied a variety of turbulent systems and tested Taylor's hypothesis using a fluorescent dye in a jet, the heated wake of a cylinder, and the atmospheric boundary layer. They were interested in the probability density function of these scalars, and found that Taylor's hypothesis worked well for conditional probability densities of the scalar fluctuations. Mi and Antonia[26] used a heated jet of air, with a turbulent intensity of about 26%, to verify different theoretical relations between spatial and temporal derivatives of temperature, corrected for finite turbulent intensities. Dahm and Southerland[27] compared 2-D spatial and spatio-temporal gradient fields of fluorescent dye in a water jet using a fast photodiode array. They found that the coherence hypothesis was only approximately verified for these fields. Piomelli, Balint, and Wallace[24] studied Taylor's hypothesis for various velocity derivatives and compared hot wire measurements, large eddy simulations, and direct numerical simulations of the Navier–Stokes equation for wall-bounded flows. Taylor's hypothesis was found to be in accord with the calculations and measurements made sufficiently far from the wall, where the mean shear is not excessive. In our experiments we have not treated the application of Taylor's hypothesis to gradients.

All hot wire measurements are sufficiently intrusive that one must compensate or otherwise adjust for the perturbations produced by the wake of the upstream probe on the velocity measured at the downstream probe. Cenedese *et al.*[23] avoided this problem by making velocity measurements with a Laser Doppler system. Only for small Δx did their correlation measurements satisfy Taylor's hypothesis very well, though admittedly I_t was rather high (13%). We discuss their results in more detail in Sec. V.

In the present experiment, Laser Doppler velocimetry is also used to measure velocity correlations, so that there is no downstream perturbation. Unlike the studies discussed above, however, we examine Taylor's hypothesis in a quasi-2-D system: a flowing soap film.

III. EXPERIMENTAL SETUP

The use of soap films as convenient systems for the experimental study of 2-D hydrodynamics began with the pioneering work of Couder and coworkers[28–30] and Gharib and Derango.[31] Our measurements are performed using a flowing soap film apparatus developed at the University of Pittsburgh by Kellay, Wu, and Goldburg,[32] and Rutgers, Wu, and

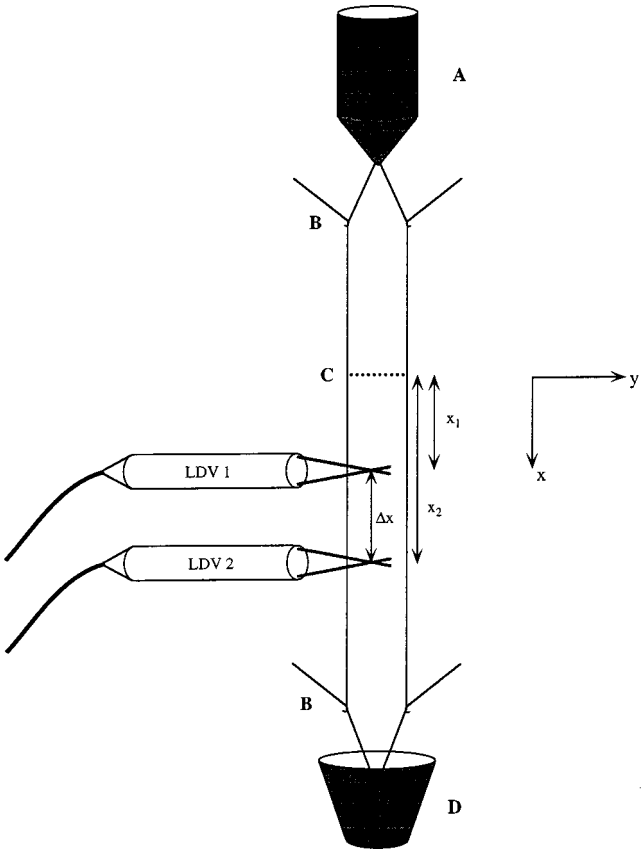

FIG. 1. A diagram of the experimental setup: (a) upper soap reservoir; (b) hooks which hold plastic wires between which soap film flows; (c) comb behind which turbulence is generated in the film; (d) lower soap reservoir. The two LDV probes which measure the velocity in the film are labeled 1 and 2. Downstream distances are labeled as referred to in the text.

Goldburg;[33,34] we are using the latest version of this system, built by Rutgers. In our setup, a thin soap film several μm thick is allowed to fall between two taut plastic wires from an upper reservoir into a lower one, see Fig. 1. The channel width is $W=6.2$ cm over a distance of 120 cm, where the measurements are performed. Quasi-two-dimensional turbulence is generated behind a comb (tooth diameter 1 mm and spacing $M=$ 3.8 mm) which perforates the film at a fixed height. The typical transit time between the comb and lower reservoir is about one second.

The turbulence generated in such a soap film decays downstream from the grid, exhibiting many aspects which agree with theories of 2-D turbulence,[29–32,35,36] though there are also some differences. It therefore seems worthwhile to evaluate the experimental situation to date. Because the lateral dimensions of soap films are many orders of magnitude larger than their thickness, there would seem to be no doubt that the vorticity can indeed be regarded as a scalar quantity, so that vortex stretching is absent.[5] This would be a key requirement for the occurrence of two-dimensional turbulence in soap films. In addition, to be able to compare with theoretical and numerical results concerning incompressible turbulence, the two-dimensional compressibility of the film should be zero. This condition is clearly not fully met, since fluctuations in film *thickness* are visible to the eye through optical interference of light reflected from the front and back faces of the film.[30,31,36] There are, however, recent experiments in which the two-dimensional divergence $D_2 \equiv \nabla_2 \cdot \mathbf{v}(x,y)$ was measured by particle imaging velocimetery.[37] In a setup very similar to ours, D_2 was measured to be 10–15% of the rms vorticity near the comb. Note also that because the velocity of peristaltic waves is orders of magnitude larger than the velocity fluctuations,[30] the film may be regarded as incompressible from the point of view of this study.

Another mitigating factor to the two-dimensionality of soap film flow is the friction between the film and the surrounding air. In experiments which placed the film in a partial vacuum (0.03 atm),[35] it was found that the energy spectrum $E(k)$ decayed for a decade in k as $E(k) \propto k^{-\zeta}$, with $\zeta = 3.3 \pm 0.3$. This exponent had the same value both under a partial vacuum and at atmospheric pressure, the main effect of removing the air being to increase the magnitude of $E(k)$ near the comb.[35] These measurements also showed that the total kinetic energy initially decayed downstream, but ultimately leveled off at some distance from the comb, which is expected theoretically for 2-D turbulence at very high Reynolds numbers.[16] If the leveling-off distance is called x^* and the corresponding time $t^* = x^*/U_0$, then all measurements reported in this paper were made at values of $t < t^*$, i.e., at distances too close to the comb for the leveling-off to be observable.

In the experimental measurements of decaying turbulence in a soap film, only the enstrophy cascade is observed, i.e., the inverse energy cascade $[E(k) \sim k^{-5/3}]$ is not, in agreement with theory.[14,16] Recently an experiment was performed by Rutgers in which turbulence was forced by an array of teeth parallel to the direction of flow.[36] There both the inverse energy cascade ($k^{-5/3}$) and the enstrophy cascade (k^{-3}) are observed. In our opinion this experiment is the most complete laboratory realization of 2-D turbulence yet realized.

Another well-studied quasi-2-D experimental system is the surface of a stratified salt solution layer which sits above an array of magnets, and is forced electromagnetically by a time-varying current. This system was first developed by Tabeling *et al.*,[38] and has been used to study 2-D mixing by Williams, Marteau, and Gollub,[39] and for 2-D turbulence by Paret, Tabeling, and coworkers.[40–42] The two main differences between this system and ours is the viscous damping at the bottom of the sublayer, and the local injection of energy which depends on the pattern of the magnetic array and the pulsed current.[39,42] However, unlike soap film turbulence, thickness variations probably do not play a role in the layered system, though surface waves may be involved in driving the flow.[41] In contrast to the majority of the soap turbulence experiments, these stratified layer experiments have only observed the inverse energy cascade where $k^{-5/3}$, which may be related to the bottom damping.[43] In relation to the study presented here, the thin layer experiments do not use Taylor's hypothesis, nor is it possible as there is no appreciable mean flow. The global electromagnetic forcing allows for a steady state to be achieved, from which statistical ensemble and spatial averages are obtained by imaging the flow on the surface.[40,42]

We use a commercial LDV system[44] to measure velocity fluctuations in the film.[45,46] The soap solution (water and 2% commercial detergent by volume) is seeded with 1 μm polystyrene spheres at a volume fraction of about 10^{-4}, and the data rate ranges from 1 to 8 kHz. At a distance $x=8$ cm below the comb, the mean and rms velocities were typically $U_0=$ 180 cm/s and $v_{\rm rms}\equiv\langle v'^2\rangle^{1/2}=24$ cm/s in the longitudinal (streamwise) direction, where $v'\equiv v-U_0$. The turbulent intensity in these experiments was $I_t\simeq 0.14$. This is the quantity which is assumed in Taylor's hypothesis to be small,[1,9] and we have explicitly chosen for our study a value of I_t which is not very small. The Reynolds number for the channel is $\mathrm{Re}_W\equiv U_0W/\nu\simeq 11{,}000$, and for the comb $\mathrm{Re}_M\equiv U_0M/\nu\simeq 700$. The viscosity of a flowing soap film is not a well established quantity; here we use $\nu=0.1$ cm^2/s as measured in a 2-D Couette viscometer by Martin and Wu.[47] Deviations from two-dimensionality caused by air friction[34] appear not to affect the turbulence for the scales of interest here.[35]

In order to test Taylor's hypothesis, two LDV heads are used at spatially separated points. Figure 1 shows the arrangement, with the downward (flow) direction defined as the x direction. One head (labeled ''LDV 1'') is kept fixed at $x_1=8$ cm below the comb, while a second head (''LDV 2'') is placed at various points ranging from $x_2=4$ to 30 cm below the comb. The two probes are horizontally aligned so that the lower probe measures the same part of the flow as the upper one, with a delay given by the transit time between them.

Because the LDV only measures velocity when there is a scatterer in its measuring volume, the two probes do not in general measure velocity simultaneously. Therefore some binning or ''simultaneity window'' Δt is needed to perform statistical comparisons: two measurements are treated as simultaneous if they occur within Δt of one another. Here we use binning windows from $\Delta t=25$ μs to 200 μs, corresponding to frequencies $1/\Delta t$ from 5 to 40 kHz, which are higher than the largest observed frequency in the velocity power spectrum. All measurements reported here are insensitive to small changes in Δt.

One of the difficulties in examining the validity of Taylor's hypothesis in decaying turbulence is that the ''small parameter'' I_t is not constant, but decreases downstream as the turbulence decays. In Fig. 2(a) we plot our turbulent intensity as a function of distance from the comb. Thus, although we measure the correlation of velocity fluctuations relative to $x_1=8$ cm, where $I_t\simeq 0.14$, the actual turbulent intensity affecting the velocity field downstream is always less than 0.14, thus tending to *improve* the correlation. This would seem to significantly complicate the matter.

How does the turbulence decay in our system? A standard result from 3-D decaying grid turbulence is that the inverse square of the turbulent intensity depends on the distance from the grid as $I_t^{-2}=A(x/M-B)^{\beta}$, where the dimensionless constants are typically found to be $A\sim 130-150$ and $B\sim 3-20$ for $\beta=1$,[48] or $A\sim 20$ and $B\sim 3.5$ for $\beta=1.25$;[22] note that B is the effective position of the origin for this scaling in units of M. Assuming that $\beta=1.25$ means that $I_t^{-1.6}$ should be a linear function of x/M; however, we find

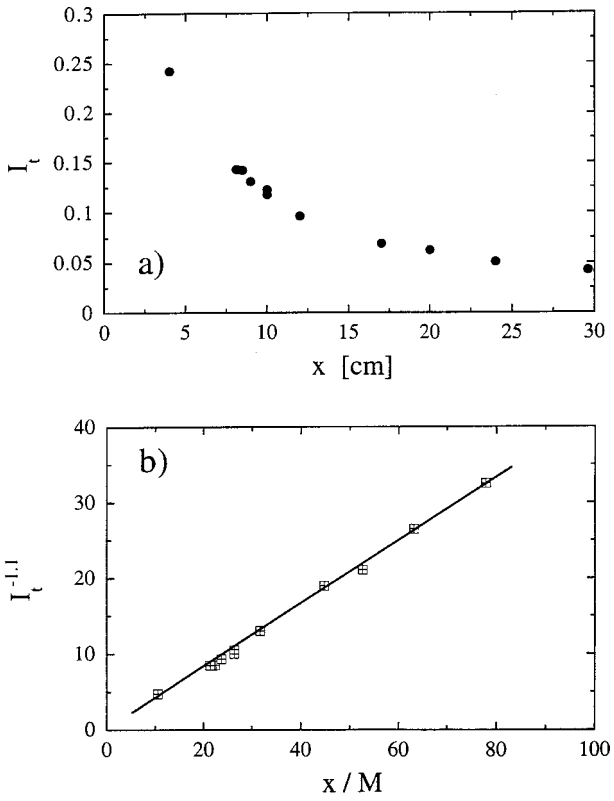

FIG. 2. The decay of the turbulent intensity I_t behind the comb in our soap film: (a) I_t versus downstream distance x; (b) the same data plotted as $I_t^{-1.1}$ vs x/M. The straight line is a linear fit (see the text).

that by taking $I_t^{-1.1}$ we get the best linear plot versus x/M, as shown in Fig. 2(b). The line corresponds to

$$\frac{1}{I_t^2}=0.2\left(\frac{x}{M}\right)^{1.8},$$

with $B=0$ for our fit, which means that the virtual origin is located at the position of the grid itself. As discussed above, we do not measure far enough downstream to see evidence of the kinetic energy saturation ($I_t\sim$const).[35]

IV. RESULTS

A. Testing the coherence hypothesis

Figure 3 shows the velocity fluctuations measured by two probes with $\Delta x=0.5$ cm. For this small separation, Taylor's hypothesis is clearly a good estimate: the two velocity traces are nearly identical except for a small shift in time, which should correspond to the transit time across the spatial separation Δx. To test whether the velocity trace is translated spatially without evolving dynamically, we measure the cross-correlation $C_{12}(\tau,\Delta x,x_1)$ between the two probes:

$$C_{12}(\tau,\Delta x,x_1)\equiv\frac{\langle v_1(x_1,t)v_2(x_1+\Delta x,t-\tau)\rangle}{v_{1\rm rms}\times v_{2\rm rms}}. \qquad (1)$$

Here $v_1(x_1,t)$ and $v_2(x_2,t)$ are the two velocities measured by the probes, $v_{i\rm rms}$ are the rms velocity fluctuations, $\Delta x\equiv x_2-x_1$, and the brackets $\langle\ \rangle$ denote a time average. Note that C_{12} is a function not only of delay time τ and separation

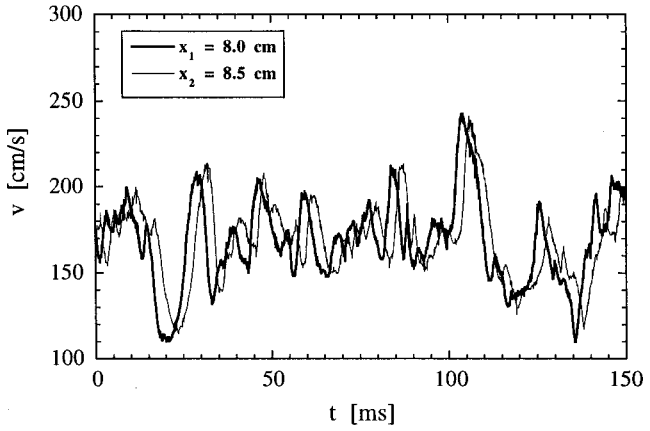

FIG. 3. Simultaneous traces of the velocity versus time at $x_1 = 8.0$ cm and $x_2 = 8.5$ cm behind the comb.

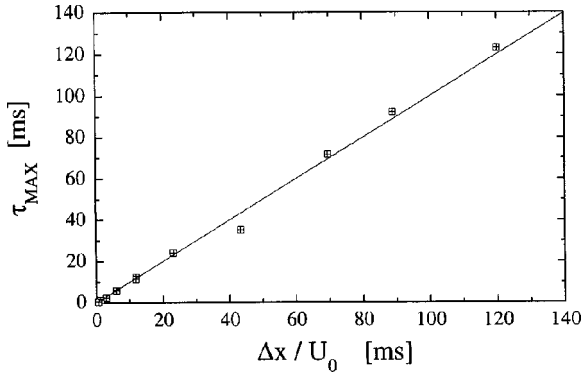

FIG. 5. The delay time τ_{MAX} for the maximum of the cross correlations in Fig. 4 versus the transit time $\Delta x/U_0$. The solid line corresponds to $\tau_{\mathrm{MAX}} = \Delta x/U_0$.

Δx, but also of the absolute location of the first probe x_1. Whereas the functional dependence on Δx includes the decay of the turbulence, the dependence on x_1 denotes the origin from which this decay is measured. Varying x_1 would permit the study of the similarity of turbulent decay at various points downstream. In this study we fix $x_1 = 8$ cm, and characterize the turbulence relative to this point.

Figure 4 shows $C_{12}(\tau,\Delta x)$ vs τ for several different separations Δx. As expected, there is a well-defined maximum correlation,

$$C_{12}^{\mathrm{MAX}}(\Delta x) \equiv C_{12}(\tau_{\mathrm{MAX}},\Delta x),$$

at a particular value of the delay time $\tau_{\mathrm{MAX}}(\Delta x)$. Taylor's coherence hypothesis requires that $C_{12}^{\mathrm{MAX}}(\Delta x)$ be close to 1, and $\tau_{\mathrm{MAX}}(\Delta x)$ be equal to the transit time $\Delta x/U_0$. Figure 5 shows τ_{MAX} as a function of $\Delta x/U_0$, in agreement with the line drawn for $\tau_{\mathrm{MAX}} = \Delta x/U_0$.[49] As predicted by Taylor's hypothesis, the slope of this line is unity. The small deviations are due to errors in our measurement of Δx.

In Fig. 6 we plot the maximum correlation $C_{12}^{\mathrm{MAX}}(\Delta x)$. As one would expect, the correlation decreases as Δx increases, though we have not found any simple functional form to fit to this decrease, nor is there to our knowledge any predicted form. The loss of correlation is due to the dynamic evolution of the velocity fluctuations and sets a limit to Taylor's hypothesis, which we quantify by defining an ''evolution length'' δ_e as the separation for which the correlation drops to 50%. For our experiment we find $\delta_e \simeq 7$ cm, corresponding to an evolution time $\tau_e = \delta_e/U_0 \simeq 40$ ms. This length is much larger than the relevant lengths of the turbulent velocity field, as we discuss in the next section. Note that the decrease in the relative turbulent intensity as Δx increases is adjusted for in the definition of C_{12}, which is normalized by the velocity fluctuations at both points. However, we cannot completely discount the possibility that this decay affects the decorrelation itself, in addition to changing the size of the fluctuations as measured by I_t in Fig. 2(a).

B. Testing Taylor's hypothesis

The statistical study of turbulence is framed in terms of velocity correlation functions, structure functions, and energy spectra; here we focus on the structure function. The longitudinal velocity difference between two points separated by a distance r is written as

$$\delta v(r,t) \equiv (\mathbf{v}(x_1+r,t) - \mathbf{v}(x_1,t)) \cdot \hat{\mathbf{r}},$$

where the unit vector $\hat{\mathbf{r}}$ is in the downward direction of the flow. The nth order structure function is defined as

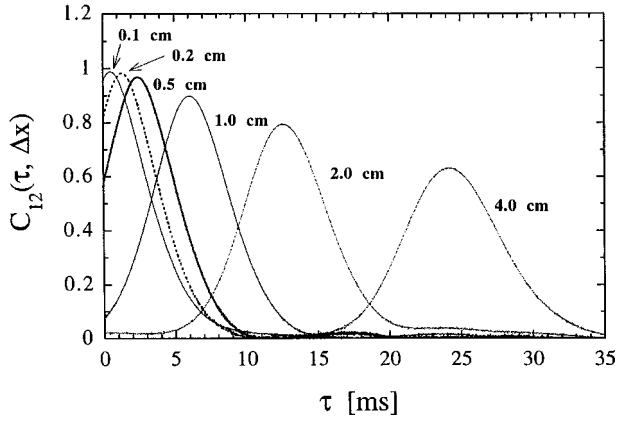

FIG. 4. The cross correlation $C_{12}(\tau,\Delta x)$ versus delay time τ for several different values of Δx (as labeled).

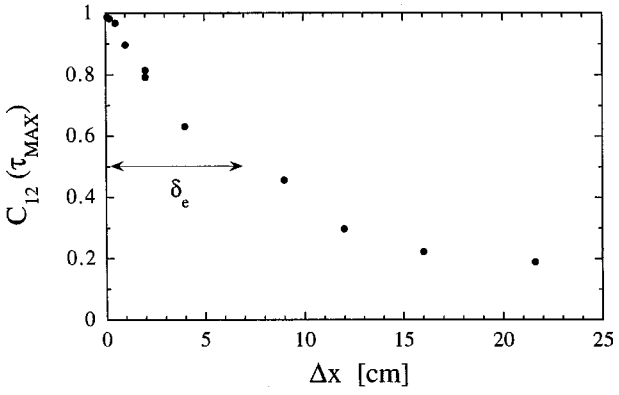

FIG. 6. The maximum value of the cross correlations in Fig. 4, C_{12}^{MAX} versus the downstream separation Δx. The arrow shows the evolution length $\delta_e \simeq 7$ cm (see the text).

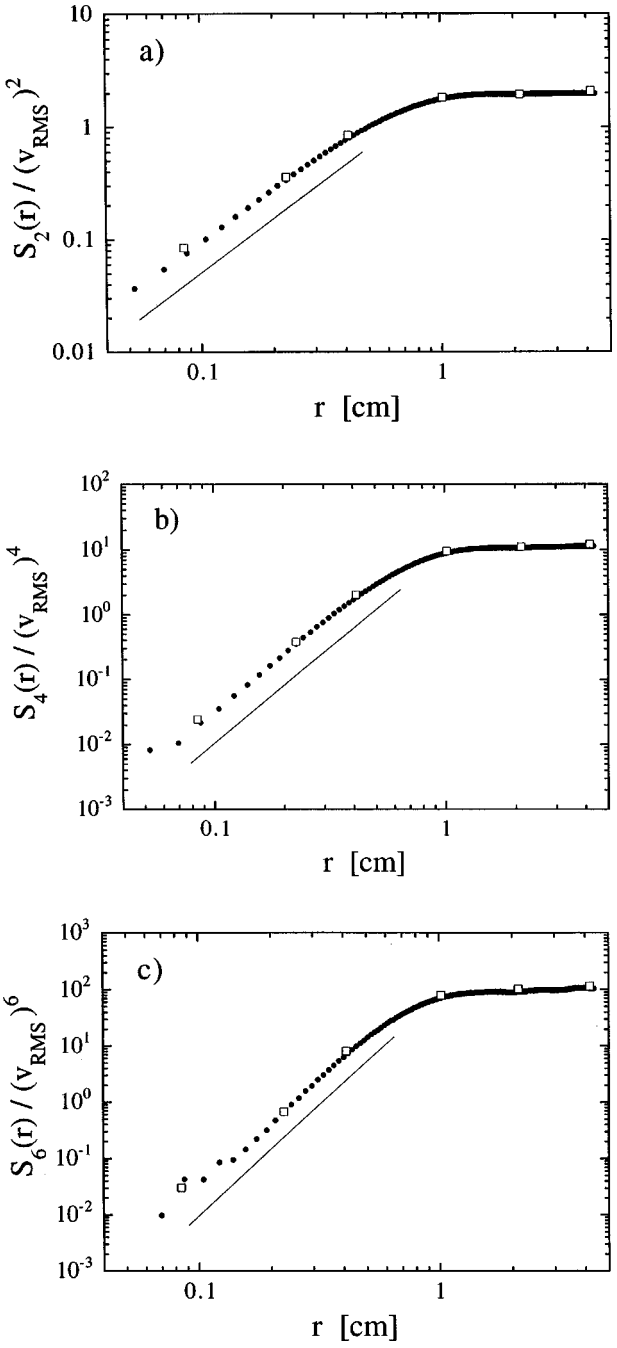

FIG. 7. Experimental check of Taylor's hypothesis for (a) second order structure function $S_2(r)$ taken at $x=8$ cm using Taylor's hypothesis; (b) fourth order structure function $S_4(r)$; (c) sixth order structure function $S_6(r)$. The open squares are direct spatial measurements made using two probes, and the lines correspond to the fitted scalings described in the text.

$$S_n(r) \equiv \langle (\delta v(r,t))^n \rangle .$$

In Fig. 7 we show the structure functions $S_2(r)$, $S_4(r)$, and $S_6(r)$, calculated from single point velocity measurements (10^5 to 10^6 data points) using Taylor's hypothesis: $r = U_0 \tau$ (solid circles). We also plot direct spatial measurements of these structure functions made using two probes (open squares). This is a direct confirmation of Taylor's statistical hypothesis, which is one of the central results of our study. Note that $S_2(r)$ shows a scaling region of about a decade where $S_2(r) \propto r^{1.6 \pm 0.2}$, in good agreement with other experiments on turbulent soap films.[50,37] We also find approximately that $S_4(r) \propto r^{2.9 \pm 0.3}$ and $S_6(r) \propto r^{4.0 \pm 0.3}$, as shown in the figure. The third moment $S_3(r)$ has been treated in detail elsewhere.[50]

For $r > 1$ cm, the $S_n(r)$ saturate to constant values, which for $S_2(r)$ is equal to $2v_{\mathrm{rms}}^2$. This occurs roughly at the integral or outer scale,[2] which characterizes the largest scales on which the velocity is correlated. The integral scale l_0 is defined as

$$l_0 \equiv \int_0^\infty b(r) dr / v_{\mathrm{rms}}^2 , \tag{2}$$

where $b(r)$ is the velocity correlation function:

$$b(r) \equiv \langle v'(x,t) v'(x+r,t) \rangle = v_{\mathrm{rms}}^2 - \tfrac{1}{2} S_2(r).$$

At $x_1 = 8$ cm we find $l_0 = 0.6$ cm, which is much less than the evolution length $\delta_e = 7$ cm. Thus for the turbulence in our soap film, Taylor's hypothesis is justified: the two signals are correlated better than 90% for scales $r < l_0$ (see Figs. 6 and 7).

Some comment should be made on the observed values of the exponents for the structure functions $S_n(r)$, which as n increases become further from $S_n(r) \propto r^n$, the theoretical expectation for the 2-D enstrophy cascade.[16,15] It is well known that in 3-D turbulence the scaling law exponents of the nth order structure functions deviate from their expected value of $n/3$ as n gets large,[3] and this systematic difference is attributed to the intermittency of the fluctuations.[5] In our case it is difficult to draw a conclusion merely from the measurement of scaling over one decade, though the measured exponents are clearly different from the predicted scaling. If these exponents are confirmed for 2-D decaying turbulence in soap films, they would indicate stronger intermittency corrections to scaling in 2D than in 3D. Some evidence of intermittency, indicated by non-Gaussian velocity fluctuations, has been previously reported in soap film turbulence,[50] and this is supported by recent numerical simulations of decaying 2-D turbulence in a channel similar to ours.[51]

C. Detailed study of the velocity decorrelation

There are in general two reasons for the breakdown of Taylor's hypothesis: the entrance of new structures into the line of travel, introducing new fluctuations into the signal, and the evolution of the velocity field itself. In Fig. 8 we show an overlay of the velocity measured at $x_1 = 8.0$ cm vs t, and the velocity measured at $x_2 = 10.0$ cm vs $t - \tau_{\mathrm{MAX}}$ ($\Delta x = 2$ cm). For a perfect correlation ($C_{12}^{\mathrm{MAX}} = 1$) the two curves would fall on top of each other. The arrows indicate fluctuations which have either appeared or disappeared during the transit time between the two probes. In effect this means that information is being generated, and this ''new information'' contributes to the velocity decorrelation (Fig. 5).

To explore the details of this process, we measure the coherence spectrum $Cs(f)$ of the fluctuations at x_1 and x_2.[52] If the coherence hypothesis were justified, then $v_1 \equiv v(x_1,t)$ would be identical to $v_2 \equiv v(x_2, t - \tau_{\mathrm{MAX}})$. If

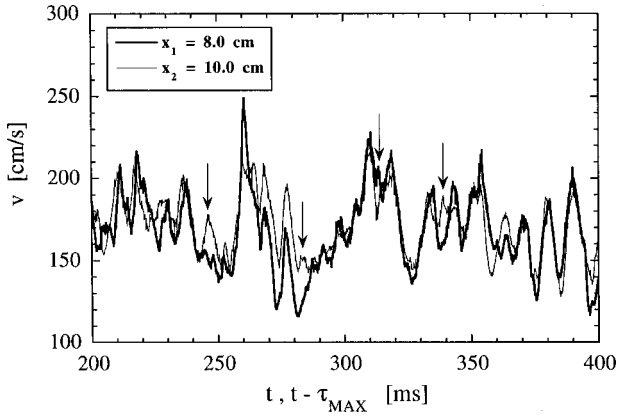

FIG. 8. Overlay of the velocity measured at $x_1 = 8.0$ cm versus t, and the velocity measured at $x_1 = 10.0$ cm versus $t - \tau_{\mathrm{MAX}}$. The arrows indicate fluctuation spikes which have either appeared or disappeared during the transit between the two probes.

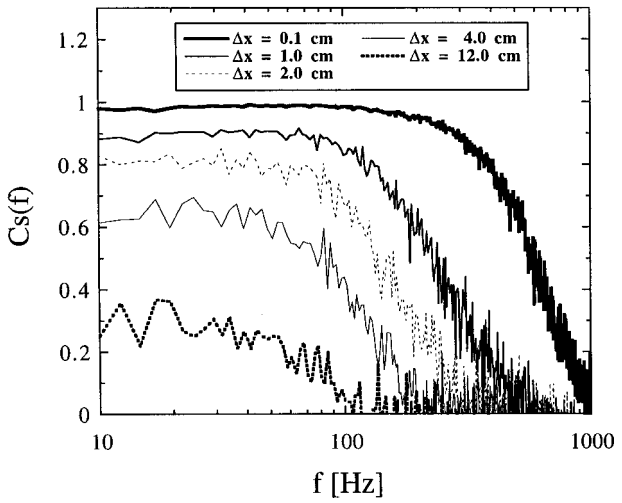

FIG. 10. Coherence spectra for several values of Δx as a linear-log plot of f.

$\hat{v}_1(f)$ is the complex Fourier transform of v_1, then the standard power spectrum is $Ps_1(f) = \langle \hat{v}_1(f)\hat{v}_1^*(f) \rangle$, where $\hat{v}^*$ is the complex conjugate of $\hat{v}$. The coherence spectrum is

$$Cs(f) \equiv \frac{1}{2} \frac{\langle \hat{v}_1(f)\hat{v}_2^*(f) + \hat{v}_1^*(f)\hat{v}_2(f) \rangle}{\sqrt{Ps_1(f) \times Ps_2(f)}}, \tag{3}$$

normalized so that $Cs = 1.0$ for frequencies where the two time series are coherent. A measurement of $Cs(f)$ with increasing probe separation shows which modes in the turbulent spectrum persist longer and which evolve faster.

Consider first the velocity power spectrum at a single point, shown as the thin line in Fig. 9. This spectrum, according to the standard picture of 2-D decaying turbulence,[15,16] should have a power law dependence $Ps(f) \sim f^{-\alpha}$ in the enstrophy cascade range, with $\alpha = 3$. In an earlier soap film experiment,[35] this exponent was found to be measurably larger than 3; here we find $\alpha = 3.6 \pm 0.2$.[53] We compare this to the coherence spectrum, which we expect to be nearly equal to 1.0 for small separations. The coherence spectrum for $\Delta x = 0.2$ cm is also shown in Fig. 9 (thick line). We see that $Cs(f)$ is indeed close to unity over most of the frequency range in which the power spectrum appears. However, the coherence drops below $Cs \sim 0.9$ at $f \sim 300$ Hz, around the middle of the range where $Ps(f) \sim f^{-\alpha}$, and for $f \sim 850$ Hz, where the power spectrum is reaching the noise floor in our measurement, $Cs \sim 0.2$. Thus already at $\Delta x = 0.2$ cm it appears that the high frequency components are the most rapidly evolving, although for the 2D enstrophy cascade it is expected that the ''eddy turnover time'' is independent of size.[14] This decrease in $Cs(f)$ may indicate viscous dissipation effects.

Figure 10 shows the $Cs(f)$ at five increasing separations Δx. In each case we see decorrelation at higher frequencies (smaller scales), while the low frequency part remains constant, and decreases as Δx increases. This constant correlation is approximately equal to $C_{12}^{\mathrm{MAX}}(\Delta x)$, which means that the overall velocity coherence is determined mainly by the low frequency components. The high frequency decorrelation moves to lower frequencies as Δx increases. To see whether the whole shape of the $Cs(f)$ follows the decay of $C_{12}^{\mathrm{MAX}}(\Delta x)$, we normalize the coherence spectra as $Cs(f)/C_{12}^{\mathrm{MAX}}$ in Fig. 11. The curves do not lie entirely on top of each other, indicating that the cutoff at high frequencies follows a different evolution than C_{12}^{MAX}. The cutoff shape is

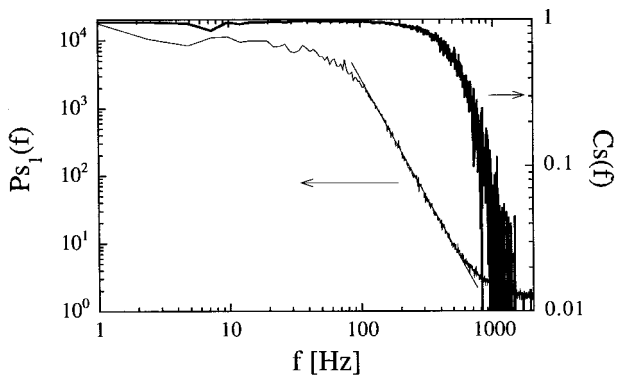

FIG. 9. A comparison of the coherence spectrum [Eq. (3)] for $\Delta x = 0.2$ cm, and the power spectrum taken at $x_1 = 8$ cm. The line is a fit to the power law $Ps_1(f) \sim f^{-\alpha}$ with $\alpha = 3.6 \pm 0.2$.

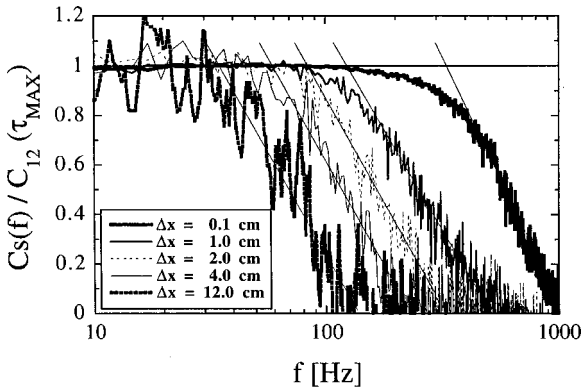

FIG. 11. Coherence spectra as in Fig. 10 normalized by the maximum cross correlation C_{12}^{MAX} from Fig. 6. The straight lines through the high frequency part of the coherence spectra corresponds to $Cs(f) \sim \log(1/f)$.

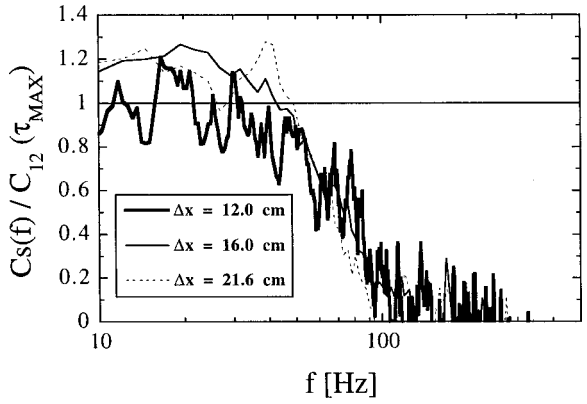

FIG. 12. Coherence spectra for several large values of Δx as a linear-log plot of f, normalized by the maximum cross correlation C_{12}^{MAX} from Fig. 6.

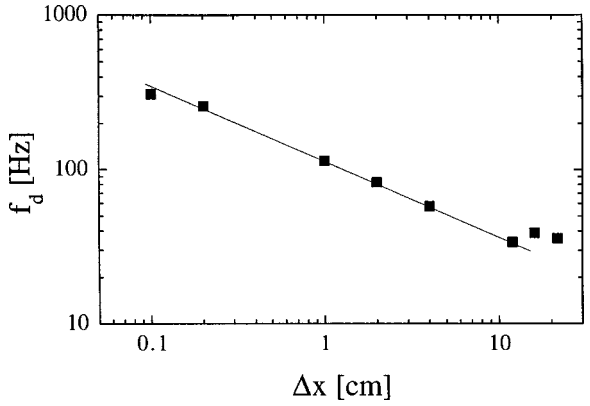

FIG. 13. The frequency scale f_d of the logarithmic decay $Cs(f)\sim\log(1/f)$ (lines in Fig. 11) versus Δx. The straight line represents the scaling $f_d \sim \Delta x^{-1/2}$.

well described as $Cs(f)\sim\log(1/f)$, shown as the straight lines drawn through the data. This advancing cutoff is reminiscent of the loss of predictability in the spectra of atmospheric turbulence simulations.[14,54]

At larger separations ($\Delta x > 12$ cm), we find that the spectral cutoff does not change with Δx. In Fig. 12 we superpose the coherence spectra for Δx from 12 to 22 cm, normalized by $C_{12}^{\mathrm{MAX}}(\Delta x)$. The curves lie reasonably on top of each other, which means that the entire coherence spectrum follows the overall decrease of C_{12}^{MAX}. By taking the intersection of the logarithmic fit with the line $Cs(f) = C_{12}^{\mathrm{MAX}}(\Delta x)$ in Figs. 11 and 12, we use the frequency f_d of the intersection to characterize the position of the spectral cutoff.[14] We plot this frequency in Fig. 13. Up to $\Delta x \simeq 12$ cm, the advance of f_d to lower frequencies is consistent with the scaling $f_d \sim \Delta x^{-1/2}$, which is slower than that seen for wave number cutoff in 2-D numerical simulations of atmospheric predictability.[14,54] For $\Delta x > 12$ cm, f_d reaches a constant value of about 30 Hz, corresponding to a length of 6 cm, which is the size of our system (the channel width $W = 6$ cm).

The loss of coherence in the velocity field is clearly due to its downstream development broadly defined, including both turbulent evolution and energy decay. We do not believe that the observed correlation loss is due to the decay in I_t, because of the way we have normalized C_{12} as discussed above, though it cannot be excluded entirely. Note that the decrease of I_t can be reduced by carrying out the entire experiment in a partial vacuum, though no change is then seen in the scaling form of $E(k)$ except at very small k.[35]

D. Turbulent predictability and the coherence hypothesis

The breakdown of the coherence hypothesis in our experiment is closely related to the question of predictability in 2-D turbulence.[54–56] The general study of predictability in turbulence (see, e.g., Refs. 14, 57, 58) is of particular importance to the weather prediction problem.[59] Here we briefly show how our analysis parallels this general framework. Note that here we are comparing a developing turbulent velocity with its initial state, whereas studies of predictability treat the diverging evolution of two nearly identical initial states. Nonetheless there are several similarities between the two.

Following Métais and Lesieur, we first define the time series of the *velocity difference*, or error time series,[54] which for our experiment is written as

$$\Delta v(\Delta x,t) \equiv v_1(x_1,t) - v_2(x_1+\Delta x, t-\tau_{\mathrm{MAX}}). \tag{4}$$

For a perfectly correlated signal this time series would be identically zero. We define the difference energy $\Delta E(\Delta x) = \langle(\Delta v(\Delta x,t))^2\rangle$, which is the second moment of Δv and thus a kinetic energy associated with the difference series; it is analogous to the error energy in predictability studies[54,60]. In Fig. 14 we plot a dimensionless ΔE, namely,

$$\rho(\Delta x) \equiv \frac{\Delta E(\Delta x)}{v_{1\mathrm{rms}}^2 + v_{2\mathrm{rms}}^2}, \tag{5}$$

as a function of the transit time $\Delta x/U_0$. The function ρ is defined to increase from 0 to 1 as Δx increases, and acts as a sort of distance function between the two velocity time histories. By comparing Eqs. (1) and (5), one sees that ρ and C_{12} are simply related.

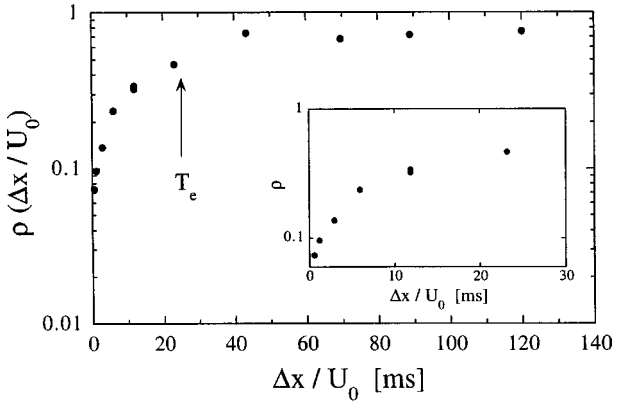

FIG. 14. The normalized error energy $\rho(\Delta x/U_0)$ as a function of time $\Delta x/U_0$ past the reference point x_1, shown as a log-linear plot. The arrow indicates the time T_e as defined in the text. Inset: an expanded view near the origin.

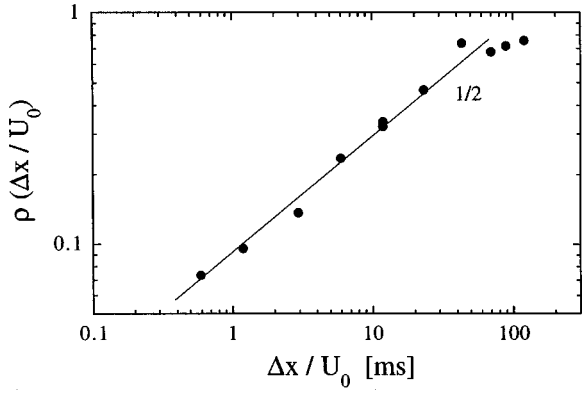

FIG. 15. A log–log plot of $\rho(\Delta x/U_0)$ as a function of downstream time $\Delta x/U_0$. The straight line corresponds to a power law dependence $(\Delta x/U_0)^{1/2}$ (see the text).

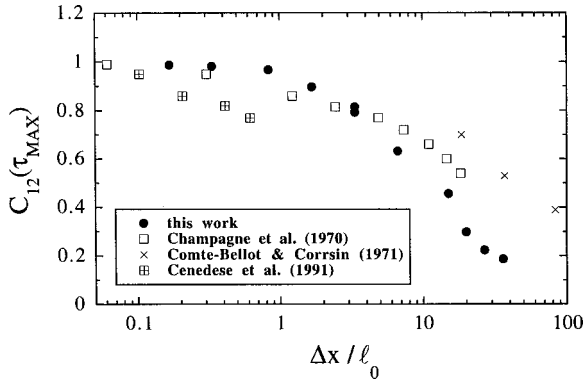

FIG. 16. A replot of C_{12}^{MAX} from Fig. 6 as a function of probe separation Δx normalized by the integral scale l_0. Also shown for comparison are 3-D results from Refs. 21, 22, and 23.

The inset to Fig. 14 shows an enlargement of $\rho(\Delta x/U_0)$ near $\Delta x/U_0=0$. There is no clear linear dependence, indicating an exponential error increase. The exponential error growth in the study of turbulent predictability is used to define a sort of Lyapunov exponent,[61] with the error energy as the metric for the distance between co-evolving turbulent states. The data shown in Fig. 14 are in fact better described by a power law $\rho\sim(\Delta x/U_0)^{1/2}$, as shown in Fig. 15. This apparent square root dependence should be interpreted only as a power law dependence: the actual value of the exponent depends on the choice of metric function, Eq. (5). Since an exponential growth of the error energy depends on the linearization of an underlying equation for ρ, Fig. 15 may indicate the presence of higher order terms, similar to the quadratic saturation term used by Lorenz to fit error growth in an iterated map.[62]

The *predictability time* T_p is a standard measure of the time beyond which the state of a turbulent system cannot be projected.[54,58] The exact value of T_p is somewhat arbitrary, though it is usually much larger than the large scale eddy turnover time for the turbulent flow.[54] We characterize the long time growth of $\rho(\tau)$ by quantifying how long the velocity v_2 remains similar to v_1. The predictability time used by Métais and Lesieur was defined by $\rho(T_p)=0.5$;[54] we define a similar time T_e such that $\rho(T_e)=0.5$, and find that $T_e\simeq 25$ ms. This is of the same order as our decorrelation time $\tau_e\simeq 40$ ms given by C_{12}^{MAX} (Fig. 6), which is not surprising given that the two functions are related.

V. DISCUSSION

A. Comparison with 3-D measurements

How do our measurements compare to similar experimental studies of 3-D decaying turbulence? Of the six studies which to our knowledge provide information comparable to Fig. 6[18–23] we will examine three in detail.[21–23] Two of these studies used hot wire anemometry,[21,22] and thus additional techniques were required to compensate for the wake of the upstream probe. Champagne *et al.*[21] used a ''grid'' made of 12 parallel channels (spacing $M'=2.54$ cm) in a wind tunnel with a mean speed of 12 m/s, and $\mathrm{Re}_{M'}=21{,}000$. Cross correlation measurements started at $x_1=$ 259 cm, where $I_t\simeq 0.018$ and $l_0\simeq 4.2$ cm. Comte-Bellot and Corrsin[22] made measurements behind a standard grid ($M=5.08$ cm) in a wind tunnel with $\mathrm{Re}_M=$ 34,000. The two hot-wire cross correlation measurements were made starting at $x_1=210$ cm, where $I_t\simeq 0.022$ and $l_0\simeq 1.1$ cm. Cenedese *et al.*[23] used a nonintrusive laser Doppler anemometer similar to our LDV (see Ref. 46), but did not use a standard grid: the turbulence was produced by a combination of a honeycomb and the channel walls. Their measurements were made in a water channel (height $h=2$ cm) starting at $x_1=$ 14 cm, where $I_t\simeq 0.13$ and $l_0\simeq 1.0$ cm. Their Reynolds numbers were also significantly lower ($\mathrm{Re}_h=4{,}800$).

Are there any differences between Taylor's hypothesis in our approximately two-dimensional soap film and in these 3D experiments? We address this question by showing $C_{12}^{\mathrm{MAX}}(\Delta x)$ from these three studies in Fig. 16 along with our measurements, plotting Δx in units of the integral scale l_0. We expect the decorrelation to occur more slowly in the soap film due to the absense of vortex stretching, and as the turbulent intensity in our experiment is high ($I_t=0.14$) compared to the two wind tunnel experiments ($I_t\sim 0.02$), our data should be directly compared only to that of Cenedese *et al.* ($I_t=0.13$). In this case the correlation in the film extends to much larger values of $\Delta x/l_0$ than in the 3-D experiment. Note that C_{12}^{MAX} from the wind tunnel experiments also extends to much larger values of $\Delta x/l_0$ than the data of Cenedese *et al.*, probably due to the fact that their turbulent intensities are much lower. More definitive conclusions would come from a single experiment (in 2D or 3D) which measures $C_{12}^{\mathrm{MAX}}(\Delta x)$ for several different I_t.

B. Detailed shape of the cross correlation $C_{12}(\tau)$

As of yet there is no rigorous underpinning to Taylor's hypothesis which would allow for the calculation of higher order corrections to velocity correlations, though an intriguing suggestion was implemented in Ref. 63. To provide detailed information for some future theory, we focus on the shape of the cross correlation function $C_{12}(\tau,\Delta x)$ around τ_{MAX}. This shape is by definition [Eq. (1)] the average con-

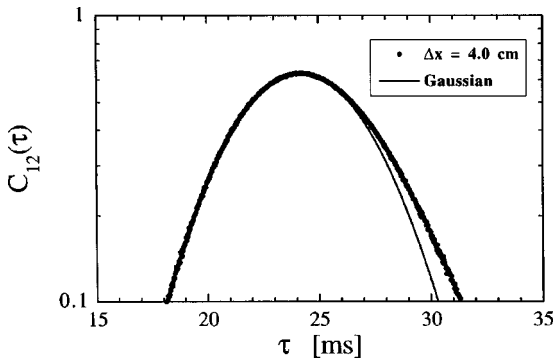

FIG. 17. Gaussian fit to the shape of $C_{12}(\tau)$ at $\Delta x = 4$ cm.

volution of a velocity fluctuation taken with itself a time τ_{MAX} later. In Fig. 17 we show as an example $C_{12}(\tau)$ for $\Delta x = 4$ cm, along with a Gaussian distribution centered on τ_{MAX}. We find that the shape is always nearly Gaussian, with a slight skewness around τ_{MAX} consistently towards the positive. The width of the Gaussian does not broaden as Δx increases, though the maximum does decrease as shown in Fig. 18. Thus the development of the cross correlation cannot be treated as a diffusion-like process, for which the width would increase as the maximum decreases. The small positive skewness is also not strongly dependent on Δx.

VI. CONCLUSION

We have presented an investigation of Taylor's hypothesis for decaying turbulence in a quasi-2-D experimental system, a flowing soap film. We have shown that for the lower order structure functions the hypothesis is a valid assumption, even when the actual cross correlation between the two probes is low. As the relevant length scale of this decorrelation is much larger than the integral scale of the turbulence ($\delta_e \gg l_0$), this phenomenon is outside the region usually considered by most studies: it is the turbulence beyond the scaling range. Information on the loss of correlation between velocities measured at upstream and downstream points, and the dependence of this effect on the dimensionality of the system, may shed light on other problems in turbulence.

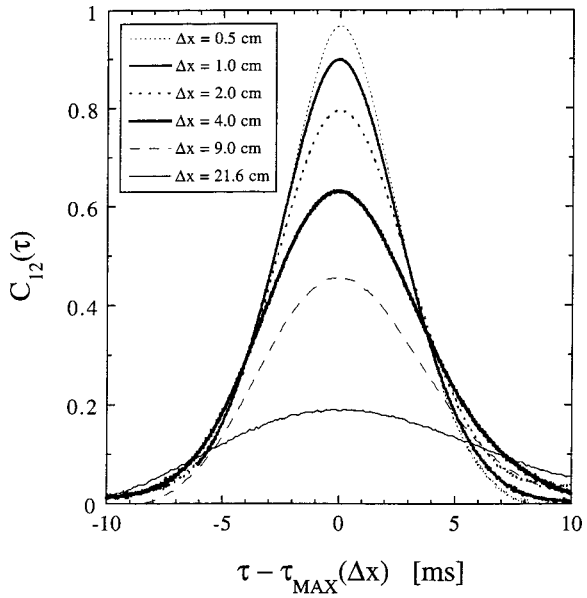

FIG. 18. An overlay of several $C_{12}(\tau)$ at various Δx (as shown), plotted versus $\tau - \tau_{MAX}$.

ACKNOWLEDGMENTS

We would like to thank M. Rivera and X. L. Wu for beneficial discussions, and H. Kellay, M. A. Rutgers, R. Cressman, and the referees for helpful comments on the manuscript. This work was supported by NASA and the National Science Foundation.

[1] G. I. Taylor, ''The spectrum of turbulence,'' Proc. R. Soc. London, Ser. A **164**, 476 (1938).
[2] A. S. Monin and A. M. Yaglom, *Statistical Fluid Mechanics* (MIT Press, Cambridge, 1975), Vol. 2.
[3] A. Arneodo, C. Baudet, F. Belin *et al.* ''Structure functions in turbulence, in various flow configurations, at Reynolds number between 30 and 5000, using extended self-similarity,'' Europhys. Lett. **34**, 411 (1996).
[4] K. R. Sreenivasan and R. A. Antonia, ''The phenomenology of small-scale turbulence,'' Annu. Rev. Fluid Mech. **29**, 435 (1997).
[5] U. Frisch, *Turbulence* (Cambridge University Press, Cambridge, 1995).
[6] V. Yakhot, ''On the relation between two-point and two-time correlation fluctuations in strong turbulence,'' preprint, 1996; ''Experiments on strong turbulence: do we really measure what we say we measure?,'' in *Flow at Ultra-High Reynolds and Rayleigh Numbers: A Status Report*, edited by R. J. Donnelly and K. R. Sreenivasan (Springer-Verlag, New York, 1998).
[7] A. N. Kolmogorov, ''The local structure of turbulence in an incompressible fluid for very large Reynolds numbers,'' Dokl. Akad. Nauk SSSR **30**, 301 (1941).
[8] A. N. Kolmogorov, ''Energy dissipation in locally isotropic turbulence,'' Dokl. Akad. Nauk SSSR **32**, 16 (1941).
[9] C. C. Lin, ''On Taylor's hypothesis and the acceleration terms in the Navier–Stokes equations,'' Q. Appl. Math. **10**, 295 (1953).
[10] J. L. Lumley, ''Interpretation of time spectra measured in high-intensity shear flows,'' Phys. Fluids **8**, 1056 (1965).
[11] H. Tennekes, ''Eulerian and Lagrangian time microscales in isotropic turbulence,'' J. Fluid Mech. **67**, 561 (1975).
[12] F. Hayot and C. Jayaprakash, ''Dynamical structure factors in models of turbulence,'' Phys. Rev. E **57**, 4867 (1998).
[13] R. Salmon, *Lectures in Geophysical Fluid Dynamics* (Oxford, New York, 1998).
[14] M. Lesieur, *Turbulence in Fluids*, 2nd ed. (Kluwer Academic, Dordrecht, 1990).
[15] R. Kraichnan, ''Inertial ranges in two-dimensional turbulence,'' Phys. Fluids **10**, 1417 (1967).
[16] G. K. Batchelor, ''Computation of the energy spectrum in homogeneous two-dimensional turbulence,'' Phys. Fluids Suppl. II **12**, 233 (1969).
[17] R. H. Kraichnan and D. Montgomery, Rep. Prog. Phys. **43**, 547 (1980).
[18] A. J. Favre, J. J. Gaviglio, and R. Dumas, ''Space–time correlations and spectra in a turbulent boundary layer,'' J. Fluid Mech. **2**, 313 (1957).
[19] A. J. Favre, J. J. Gaviglio, and R. Dumas, ''Further space–time correlations of velocity in a turbulent boundary layers,'' J. Fluid Mech. **3**, 344 (1958).
[20] M. J. Fisher and P. O. A. L. Davies, ''Correlation measurements in a non-frozen pattern of turbulence,'' J. Fluid Mech. **18**, 97 (1964).
[21] F. H. Champagne, V. G. Harris, and S. Corrsin, ''Experiments on nearly homogeneous turbulent shear flow,'' J. Fluid Mech. **41**, 81 (1970).
[22] G. Comte-Bellot and S. Corrsin, ''Simple Eulerian time correlation of full- and narrow-band velocity signals in grid-generated, 'isotropic' turbulence,'' J. Fluid Mech. **48**, 273 (1971).
[23] A. Cenedese, G. P. Romano, and F. DiFelice. ''Experimental testing of Taylor's hypothesis by L. D. A. in highly turbulent flow,'' Exp. Fluids **11**, 351 (1991).
[24] U. Piomelli, J.-L. Balint, and J. M. Wallace, ''On the validity of Taylor's hypothesis for wall-bounded flows,'' Phys. Fluids A **1**, 609 (1989).
[25] P. Kailasnath, K. R. Sreenivasan, and J. R. Saylor, ''Conditional scalar dissipation rates in turbulent wakes, jets, and boundary layers,'' Phys. Fluids A **5**, 3207 (1993).

[26]J. Mi and R. A. Antonia, ''Corrections to Taylor's hypothesis in a turbulent circular jet,'' Phys. Fluids **6**, 1548 (1994).
[27]W. J. A. Dahm and K. B. Southerland, ''Experimental assessment of Taylor's hypothesis and its applicability to dissipation estimates in turbulent flows,'' Phys. Fluids **9**, 2101 (1997).
[28]Y. Couder, ''The observation of a shear flow instability in a rotating system with a soap membrane,'' J. Phys. (France) Lett. **42**, 429 (1981).
[29]Y. Couder, ''Two-dimensional grid turbulence in a thin liquid film,'' J. Phys. (France) Lett. **45**, 353 (1984).
[30]Y. Couder, J.-M. Chomaz, and M. Rabaud, ''On the hydrodynamics of soap films,'' Physica D **37**, 384 (1989).
[31]M. Gharib and P. Derango, ''A liquid film (soap film) tunnel to study two-dimensional laminar and turbulent shear flows,'' Physica D **37**, 406 (1989).
[32]H. Kellay, X. L. Wu, and W. I. Goldburg, ''Experiments with turbulent soap films,'' Phys. Rev. Lett. **74**, 3975 (1995).
[33]W. I. Goldburg, M. A. Rutgers, and X. L. Wu, ''Experiments on turbulence in soap films,'' Physica A **239**, 340 (1997).
[34]M. A. Rutgers, X. L. Wu, R. Bagavatula, A. A. Peterson, and W. I. Goldburg, ''Two-dimensional velocity profiles and laminar boundary layers in flowing soap films,'' Phys. Fluids **8**, 2847 (1997).
[35]B. Martin, X. L. Wu, W. I. Goldburg, and M. A. Rutgers, ''Spectra of decaying turbulence in a soap film,'' Phys. Rev. Lett. **80**, 3964 (1998).
[36]M. A. Rutgers, ''Forced 2D turbulence: experimental evidence of simultaneous inverse energy and forward enstrophy cascades,'' Phys. Rev. Lett. **81**, 2244 (1998).
[37]M. Rivera, P. Vorobieff, and R. E. Ecke, ''Turbulence in flowing soap films: Velocity, vorticity, and thickness fields,'' Phys. Rev. Lett. **81**, 1417 (1998).
[38]P. Tabeling, S. Burkhart, O. Cardoso, and H. Willaime, ''Experimental study of freely decaying two-dimensional turbulence,'' Phys. Rev. Lett. **67**, 3772 (1991).
[39]B. S. Williams, D. Marteau, and J. P. Gollub, ''Mixing of a passive scalar in a magnetically forced two-dimensional turbulence,'' Phys. Fluids **9**, 2061 (1997).
[40]J. Paret and P. Tabeling, ''Experimental observation of the two-dimensional inverse energy cascade of energy,'' Phys. Rev. Lett. **79**, 4162 (1997).
[41]J. Paret, D. Marteau, O. Paireau, and P. Tabeling, ''Are flows electromagnetically forced in thin stratified layers two-dimensional?,'' Phys. Fluids **9**, 3102 (1997).
[42]J. Paret and P. Tabeling, ''Intermittency in the two-dimensional inverse cascade of energy: Experimental observations,'' Phys. Fluids **10**, 3126 (1998).
[43]Very recently Paret, Jullien, and Tabeling have reported the observation of the direct enstrophy cascade in the salt solution layer experiment, including k^{-3} and other aspects [J. Paret, M-C. Jullien, and P. Tabeling, ''Vorticity statistics in the two-dimensional enstrophy cascade,'' Phys. Rev. Lett. **83**, 3418 (1999)]. However, in this case they do not observe the inverse energy cascade, or any $k^{-5/3}$ scaling in the spectrum; to date the only observation of both cascades has been in the driven soap film experiment of Rutgers (Ref. 36). Both soap film and stratified layer experiments continue to provide new insights into 2-D turbulence.
[44]We are using two 9253-120 fiberoptic LDV probes, a Colorlink 9230, and an IFA 655 correlator from TSI Inc., P. O. Box 64204, St. Paul, MN 55164.
[45]F. Durst, A. Melling, and J. H. Whitelaw, *Principles and Practice of Laser-Doppler Anemometry*, 2nd ed. (Academic, New York, 1981).
[46]P. Buchhave, W. K. George, and J. Lumley, ''The measurement of turbulence with the laser-Doppler anemometer,'' Annu. Rev. Fluid Mech. **11**, 443 (1979).
[47]B. Martin and X. L. Wu, ''Shear flow in a two-dimensional Couette cell: A technique for measuring the viscosity of free-standing liquid films,'' Rev. Sci. Instrum. **66**, 5603 (1995).
[48]G. K. Batchelor and A. A. Townsend, ''Decay of isotropic turbulence in the initial period,'' Proc. R. Soc. London, Ser. A. **193**, 539 (1948).
[49]For these calculations we recalculate U_0 for each Δx as the average of $\langle v_1(x_1,t)\rangle$ and $\langle v_2(x_2,t)\rangle$.
[50]A. Belmonte, W. I. Goldburg, H. Kellay, M. A. Rutgers, B. Martin, and X. L. Wu, ''Velocity fluctuations in a turbulent soap film: The third moment in two dimensions,'' Phys. Fluids **11**, 1196 (1999).
[51]C. H. Bruneau, O. Greffier, and H. Kellay, ''Numerical studies of grid turbulence in two dimensions and comparison with experiments on turbulent soap films,'' Phys. Rev. E **60**, 1162 (1999).
[52]G. M. Jenkins and D. G. Watts, *Spectral Analysis and its Applications* (Holden-Day, San Francisco, 1968), Chap. 8.
[53]Note that this does not necessarily contradict the scaling for $S_2(r)$, as the *width* of a scaling range in $E(k)$ can reduce the scaling exponent, by effectively introducing other length scales: the bounds of the scaling region [A. Babiano, C. Basdevant, and R. Sadourny, ''Structure functions and dispersion laws in two-dimensional turbulence,'' J. Atmos. Sci. **42**, 941 (1985)].
[54]O. Métais and M. Lesieur, ''Statistical predictability of decaying turbulence,'' J. Atmos. Sci. **43**, 857 (1986).
[55]C. E. Leith, ''Atmospheric predictability and two-dimensional turbulence,'' J. Atmos. Sci. **28**, 145 (1971).
[56]S. Kida, M. Yamada, and K. Ohkitani, ''Error growth in a decaying two-dimensional turbulence,'' J. Phys. Soc. Jpn. **59**, 90 (1990).
[57]C. E. Leith and R. H. Kraichnan, ''Predictability of turbulent flows,'' J. Atmos. Sci. **29**, 1041 (1972).
[58]E. Aurell, G. Boffetta, A. Crisanti, G. Paladin, and A. Vulpiani, ''Growth of noninfinitesimal perturbations in turbulence,'' Phys. Rev. Lett. **77**, 1262 (1996).
[59]*Turbulence and Predictability in Geophysical Fluid Dynamics and Climate Dynamics*, edited by M. Ghil, R. Benzi, and G. Parisi (North-Holland, Amsterdam, 1985).
[60]G. Bofetta, A. Celani, A. Crisanti, and A. Vulpiani, ''Predictability in two-dimensional decaying turbulence,'' Phys. Fluids **9**, 724 (1997).
[61]J.-P. Eckmann and D. Ruelle, ''Ergodic theory of chaos and strange attractors,'' Rev. Mod. Phys. **57**, 617 (1985).
[62]E. N. Lorenz, ''The growth of errors in prediction,'' in Ref. 61.
[63]J.-F. Pinton and R. Labbé, ''Correction to the Taylor hypothesis in swirling flows,'' J. Phys. II **4**, 1461 (1994).